Dominance mechanisms in supergene alleles controlling butterfly wing pattern variation: insights from gene expression in Heliconius numata

Héloïse Bastide, Suzanne Saenko, Mathieu Chouteau, Mathieu Joron, Violaine Llaurens

Title:

Dominance mechanisms in supergene alleles controlling butterfly wing pattern variation: Insights from gene expression in *Heliconius numata*

Héloïse Bastide[1], Suzanne V. Saenko[1], Mathieu Chouteau[2,3], Mathieu Joron[2] and Violaine Llaurens[1]

[1]Institut de Systématique, Evolution et Biodiversité (UMR 7205 CNRS, MNHN, Sorbonne Université, Université des Antilles) Muséum National d'Histoire Naturelle - CP50, 57 rue Cuvier, 75005 Paris, France

[2] CEFE, Université de Montpellier, CNRS, EPHE, IRD, Montpellier, France

[3]Laboratoire Ecologie, Evolution, Interactions Des Systèmes Amazoniens (LEEISA), USR 3456, Université De Guyane, CNRS Guyane, 275 route de Montabo, 97334 Cayenne, French Guiana

Corresponding author: Héloïse Bastide

Current address : Laboratoire Évolution, Génomes, Comportement et Écologie, CNRS, IRD, Université Paris-Saclay – Institut Diversité, Écologie et Évolution (IDEEV), 12 route 128, 91190 Gif-sur-Yvette, France

Tel. : +33 (0)1 69 15 45 39

e-mail: heloise.bastide@universite-paris-saclay.fr

Running Title: Genetic dominance in wing color pattern variations

Word count: 4700

Abstract:

Loci under balancing selection, where multiple alleles are maintained, offer a relevant opportunity to investigate the role of natural selection in shaping genetic dominance: the high frequency of heterozygotes at these loci has been shown to enable the evolution of dominance among alleles. In the butterfly *Heliconius numata*, mimetic wing colour variations are controlled by an inversion polymorphism of a circa 2 Mb genomic region (supergene *P*), with strong dominance between sympatric alleles. To test how differences in dominance observed on wing patterns correlate with variations in expression levels throughout the supergene region, we sequenced the complete transcriptome of heterozygotes at the prepupal stage and compared it to corresponding homozygotes. By defining dominance based on non-overlapping ranges of transcript expression between genotypes, we found contrasting patterns of dominance between the supergene and the rest of the genome; the patterns of transcript expression in the heterozygotes were more similar to the expression observed in the dominant homozygotes in the supergene region. Dominance also differed among the three subinversions of the supergene, suggesting possible epistatic interactions among their gene contents underlying dominance evolution. We found the expression pattern of the melanization gene *cortex* located in the *P*-region to predict wing pattern phenotype in the heterozygote. We also identify new candidate genes that are potentially involved in mimetic colour pattern variations highlighting the relevance of transcriptomic analyses in heterozygotes to pinpoint candidate genes in non-recombining regions.

Introduction:

Dominance between alleles determines the phenotype of heterozygotes and plays a key role in the evolutionary fate of alleles. Indeed, new adaptive variants are often dominant, because emerging alleles, initially at rare frequency within population, are more prone to be picked up by positive selection when expressed at heterozygous state (Haldane 1956). On the contrary, deleterious variants are generally recessive, because they escape purging if they are scarcely expressed (Charlesworth and Charlesworth 1999; Charlesworth and Willis 2009; Connallon and Hall 2018). In loci under balancing selection, where multiple alleles are maintained in sympatry, heterozygotes are frequent and natural selection thus frequently acts on heterozygotes, promoting the evolution of dominance (Otto and Bourguet 1999; Llaurens et al. 2009). Dominance can arise as an inherent property of the encoded protein, but can also be tuned by expression modifiers, especially in polymorphic loci (Wilkie 1994). At the translational level, one of the two protein copies in the heterozygote could be dis- or nonfunctional due to non-synonymous or missense mutations in the coding DNA sequence, such as the recessive O allele in the ABO blood group system (Yamamoto et al. 1990). At the transcriptional level, recessivity can arise from differences of overall level of expression of a gene between homozygotes, skewing the phenotype of the heterozygotes toward that of the allele with the higher expression. This is most clearly seen in cases of regulatory mutations, which can affect the expression of a gene in a particular tissue. For example, mutations at a regulatory element located 5-kb upstream of the *tan* gene in *Drosophila erecta* suppresses dark pigmentation in the abdomen of homozygous light females, but heterozygotes have pigmentation similar to homozygous dark females (Yassin et al. 2016). The regulatory mutations can also be part of the RNA transcripts, leading to allele-specific differential expression in the heterozygotes, such as in the case of the self-incompatibility locus in *Arabidopsis halleri* and *A. lyrata* where small RNAs specifically repress some alleles at the *SCR* gene (Durand et al. 2014). Remarkably, all these diverse molecular mechanisms are maintained by balancing selection, allowing selection to act on the phenotype of the heterozygotes, and therefore shaping the

evolution of dominance (see Billiard et al. 2021 for a review). Both levels of gene and allele expression can trigger dominance in heterozygotes and be submitted to selection in polymorphic loci where heterozygotes have a high frequency.

The neo-tropical butterfly *Heliconius numata* is a fascinating example of adaptive polymorphism within populations, with multiple mimetic wing color patterns maintained in sympatry. These different wing patterns are submitted to strong natural selection exerted by predators favoring mimicry towards distinct toxic species (Joron et al. 1999). In this species, the discrete variations in wing colour pattern are mainly controlled by the supergene *P* (Joron et al. 2006). The dissection of the supergene architecture is still in progress but, among the 129 genes located within the 2 Mb long supergene (Jay et al. 2018), the gene *cortex* is known to control variations in hindwing melanic patterns in *H. numata* (Nadeau et al. 2016; Livraghi et al. 2020). A number of other genes at the supergene are likely to control variations of other individual pattern elements (Saenko et al. 2019). Combinations of allelic variants at multiple linked genes will thus give rise to differentiated haplotypes at the supergene *P*, each governing distinct wing pattern features (Joron et al. 2006). By comparing the phenotypes of homozygotes and heterozygotes at the supergene, strong dominance between supergene alleles have been found in sympatry, whereas mosaics of dominance resulting in intermediate phenotypes were observed in heterozygotes obtained from crosses performed with individuals from different populations (Le Poul et al. 2014). Natural selection promoting mimicry favors coordinated dominance between supergene alleles found in sympatry, resulting in mimetic phenotypes expressed in heterozygotes (Le Poul et al. 2014; Arias et al. 2016). The mimicry in heterozygotes may stem from either the dominance of the derived mimetic alleles (*i.e.* Haldane's sieve) or the modification of dominance of the ancestral alleles (Llaurens et al. 2015). Moreover, supergene alleles are characterized by different chromosomal inversions favoring their genetic differentiation (Joron et al. 2011), and alleles exhibiting the ancestral gene order are recessive to alleles exhibiting a rearranged gene order, the latter being introduced into *H. numata* via introgression from a closely-related species (Jay et al.

2018). We thus aim at understanding the molecular mechanisms involved in dominance between supergene alleles, which are likely shaped by natural selection through mimicry.

In this paper, we thus compare the level of gene expression between individuals carrying either homozygous or heterozygous genotypes at the supergene *P*. We focus on two supergene alleles controlling the *bicoloratus* and *tarapotensis* phenotypes respectively. These two phenotypes are frequently observed in sympatry, and are mimetic to different communities of defended species, including the chemically-defended Ithominii species *Melinaea mothone* (*bicoloratus* mimicry ring) and *Melinaea menophilus* ssp. nov. (*tarapotensis* mimicry ring) (Joron et al. 1999). These two alleles are therefore under strong selection favouring mimicry to their respective communities (Chouteau et al. 2016). Heterozygotes P_{bic} / P_{tar} exhibit the *bicoloratus* phenotype so that the allele *bicoloratus* (referred to as P_{bic} hereafter) is dominant over the allele *tarapotensis* (P_{tar} hereafter) (Le Poul et al. 2014); Figure 1A). Increased predation has been observed on intermediate phenotypes between *tarapotensis* and *bicoloratus* (Arias et al. 2016), therefore favouring dominance in heterozygotes P_{bic} / P_{tar}. Both alleles have derived gene orders, inferred from the discrepancy in synteny with closely-related *Heliconius* species (Joron et al. 2011). The *bicoloratus* allele (P_{bic}) displays a single inversion (P_1) while the *tarapotensis* allele (P_{tar}) is thought to derive from a haplotype carrying a P_1 inversion followed by two subsequent inversions P_2 and P_3 (Joron et al. 2011). As a result, the two alleles have the same gene order at the 400-kb long P_1 inversion harboring the *cortex* gene and have different gene order at the circa 1.6-Mb long P_2-P_3 inversions (Figure 1B). Because selection on phenotypic dominance between these two alleles is well documented, this stresses the need to investigate the molecular mechanisms underlying their genetic dominance.

Given that inversions limit recombination in the supergene region, the identification of candidate genes associated to wing pattern variations through widely used association analyses (e.g., GWAS, see Jay et al. 2022) or classical QTL mapping is difficult. Analysis of transcriptomic variation could overcome such difficulties because changes in expression levels among genes

within the inversion could more likely associate with phenotypic differences than to their physical linkage. Using an RNAseq approach, we compared gene expression in the homozygotes (P_{bic} / P_{bic} and P_{tar} / P_{tar}) and heterozygotes (P_{bic} / P_{tar}) and specifically tested for departure from additivity. We focused our analyses only on transcripts where the range of expression levels did not overlap between P_{bic} / P_{bic} and P_{tar} / P_{tar} genotypes. By focusing on genes with contrasted levels of transcript expression in the homozygotes, we were thus able to compare patterns of dominance between the supergene and the rest of the genome.

Materials and Methods:

Samples, library sequencing, and *de novo* transcriptome assembly

The *H. numata* butterflies used in this study come from controlled crosses performed with individuals sampled around Tarapoto (Peru). Crosses were carried out among individuals with different genotypes at the colour pattern supergene *P* (and therefore different wing colour patterns). Individuals studied here all belong to the F2 generation of a single initial cross between a female with genotype P_{bic} / P_{arc} and a male with genotype P_{tar} / P_{aur}. The alternative alleles P_{arc} and P_{aur} control for the *arcuella* and *aurora* phenotypes that visually differ from *bicoloratus* and *tarapotensis*. These two alternative alleles have the same gene order than P_{tar} (*i.e.* they all have the three subinversions). The genotypes of the offspring were established using allele-specific primers followed by Sanger sequencing of the amplified fragments, as described in Saenko et al. 2019, therefore checking for recombinant haplotypes. We selected individuals with different combinations of P_{bic} and P_{tar} alleles from different crosses performed between F1 offspring with the relevant genotypes. The P_{bic} allele is associated with the *bicoloratus* form being dominant to the P_{tar} allele associated with *tarapotensis*, as described in Saenko et al. (2019). Forewing and hindwing wing discs were dissected from prepupae, a stage described as the key timing of expression of genes involved in colour pattern development in *Heliconius* (Martin et al. 2012). Nevertheless, our experiment does not cover the whole timeframe of wing development, so that we cannot rule out

that other genes involved in colour pattern variations located in the *P*-supergene would be differentially expressed at other developmental stages not studied here. Ten individuals were selected, including 4 individuals with the genotypes P_{bic} / P_{bic}, 3 with P_{bic} / P_{tar} and 3 with P_{tar} / P_{tar}. The reference transcriptome used in this study was assembled by Saenko et al. (2019) based on transcripts expressed in the wing discs at the 24h and prepupal stages of 24 *H. numata* samples. Total RNA was extracted and cDNA libraries prepared and sequenced as described in Saenko et al. 2019. As reported in this paper, a mean of 42 ± 15 million passing Illumina quality filter reads was obtained for each sample. Raw data were filtered for low-quality reads (<Q30) with Prinseq v0.19.5 (Schmieder and Edwards 2011), for adaptor sequences with Cutadapt v1.16 (Martin 2011) and for ribosomal RNA-like sequences with riboPicker v1.0.0 (Schmieder et al. 2012). The filtered reads were finally combined to generate a *de novo* reference transcriptome using Trinity r20140717 (Haas et al. 2013) with the following parameters: SS_lib_type = F, kmer_size = 25, max_pct_stdev = 100, minimum contig length = 200 bp. Of the 53719 transcripts of this reference transcriptome (obtained from all transcripts of the 24 afore-mentioned *H. numata* samples), 52525 are expressed in the prepupal stage. Of these, 50075, 51181 and 49808 were expressed in the P_{bic} / P_{bic} homozygotes, P_{bic} / P_{tar} heterozygotes and P_{tar} / P_{tar} homozygotes, respectively.

Estimating levels of dominance of the *bic* allele in heterozygotes using read counts (*D*)

The supergene allele P_{bic} is strongly dominant over the supergene allele P_{tar}, because P_{bic} / P_{tar} heterozygotes almost have the same wing color pattern as the P_{bic} / P_{bic} homozygotes (Figure 1A). Therefore, in the heterozygotes P_{bic} / P_{tar} we generally expect the level of expression of the genes involved in determining wing patterns to be similar to the expression in the P_{bic} / P_{bic} homozygotes. Each wing pattern allele is associated with chromosomal rearrangements at the supergene involving one inversion (rearrangement P_1 associated with the form *bicoloratus*) or two inversions (rearrangements P_1, P_2 and P_3 in *tarapotensis*; Figure 1B). The ancestral chromosomal arrangement, without any inversion, is absent from our crosses. To test whether the expression at

the supergene in heterozygotes P_{bic} / P_{tar} matches the expression observed in the P_{bic} / P_{bic} homozygotes, we compared patterns of expression between P_{bic} / P_{tar} heterozygotes and the two corresponding homozygotes in terms of gene level of expression (*D*) along the genome.

All reads were aligned to the *de novo* transcriptome using Bowtie2 v2.1.0 with default parameters (Langmead and Salzberg 2012) and read counts were calculated with samtools idxstats (Li et al. 2009). To avoid any bias due to alternative splicing, all transcripts from a single gene were annotated and the read counts estimated separately. When they existed, orthologs were identified in the closely-related species *H. melpomene* by aligning the transcripts to the Hmel2_cds and HMEL2_scaffolds databases (downloaded from Lepbase v4 (Challi et al. 2016)) with NCBI BLASTn. This, however, has revealed that the number of assembled transcripts exceeded the number of transcripts in *H. melpomene* CDS. The higher number of transcripts in our assembly may be due to variations in alternative splicing between the two species and/or an incomplete annotation for *H. melpomene* (Saenko et al. 2019). Consequently, several *numata* transcripts mapped to *melpomene* intergenic regions. Read counts were normalized using the mean and standard deviation of all reads in the transcriptome per sample. Because of the small sample size in this study, reliance on mean expression level among samples belonging to each genotype (as in Saenko et al. 2019) could strongly be biased by outliers. To avoid this problem, only transcripts with no overlap in the levels of expression between the samples of each homozygous genotype were considered for further analyses. We thus selected transcripts for which *i.e.* the maximum read count among replicates of one homozygous genotype was inferior to the minimum read count of the alternative homozygous genotype. For those selected transcripts, dominance in heterozygotes was identified by comparing the number of counts in homozygotes and heterozygotes and then associating a score *D* ranging from -3 to 3. This dominance score *D* crucially depends on the direction of the difference in the level of expression between the two homozygous genotypes (Figure 2): either the transcript is more highly expressed in P_{bic} / P_{bic} than in P_{tar} / P_{tar} homozygotes, or the other way around. We named N_i the read count of the transcripts in the different replicates of the genotype *i* and define the

dominance score D depending on the distribution of the reads counts in the homozygotes where the transcript is highly vs. lowly expressed (N_{high} and N_{low} respectively). In transcripts where the minimum counts observed in P_{bic} / P_{bic} homozygotes replicates is strictly above the maximum count among P_{tar} / P_{tar} homozygotes, we define $N_{high} = N_{Pbic\,/\,Pbic}$ and $N_{low} = N_{Ptar\,/\,Ptar}$ (category 1). Symmetrically, in transcripts where the minimum count of a transcript among P_{tar} / P_{tar} homozygotes is strictly above its maximum count among P_{bic} / P_{bic} homozygotes, we define $N_{high} = N_{Ptar\,/\,Ptar}$ and $N_{low} = N_{Pbic\,/\,Pbic}$ (category 2). The dominance score D is then defined as follows for both categories:

$D = 3$ when overdominance of the *bic* allele is observed, *i.e.* when Min ($N_{Pbic\,/\,Ptar}$) > Max (N_{high}) in category 1 or when Max ($N_{Pbic\,/\,Ptar}$) < Min (N_{low}) in category 2.

$D = 2$ when strict dominance of the *bic* allele is observed, *i.e.* when Min ($N_{Pbic\,/\,Ptar}$) > [(Min (N_{high}) + Max (N_{low})] / 2 and Min ($N_{Pbic\,/\,Ptar}$) ≤ Max (N_{high}) in category 1 or when Max ($N_{Pbic\,/\,Ptar}$) < [(Min (N_{high}) + Max (N_{low})] / 2 and Max ($N_{Pbic\,/\,Ptar}$) ≥ Min (N_{low}) in category 2.

$D = 1$ when incomplete dominance of the *bic* allele is observed, *i.e.* when Max ($N_{Pbic\,/\,Ptar}$) ≤ Min (N_{high}) and Min ($N_{Pbic\,/\,Ptar}$) > [(Min (N_{high}) + Max (N_{low})] / 2 in category 1 or when Min ($N_{Pbic\,/\,Ptar}$) ≥ Max (N_{low}) and Max ($N_{Pbic\,/\,Ptar}$) < [(Min (N_{high}) + Max (N_{low})] / 2 in category 2.

$D = 0$ when codominance of the two alleles is observed, *i.e.* when the range of expression levels observed in the heterozygotes overlap the midpoint of the range of expression observed in both homozygotes.

$D = -1$, when incomplete recessiveness of the *bic* allele is observed, *i.e.* when Min ($N_{Pbic\,/\,Ptar}$) ≥ Max (N_{low}) and Max ($N_{Pbic\,/\,Ptar}$) < [(Min (N_{high}) + Max (N_{low})] / 2 or when Max ($N_{Pbic\,/\,Ptar}$) ≤ Min (N_{high}) and Min ($N_{Pbic\,/\,Ptar}$) > [(Min (N_{high}) + Max (N_{low})] / 2 in category 2.

D = -2, when strict recessivity of the *bic* allele is observed, *i.e.* when Max ($N_{Pbic\ /\ Ptar}$) < [(Min (N_{high}) + Max (N_{low})] / 2 and Max ($N_{Pbic\ /\ Ptar}$) ≥ Min (N_{low}) or when Min ($N_{Pbic\ /\ Ptar}$) > [(Min (N_{high}) + Max (N_{low})] / 2 and Min ($N_{Pbic\ /\ Ptar}$) ≤ Max (N_{high}) in category 2. D = -3, when underdominance of the *bic* allele is observed, *i.e.* when Max ($N_{Pbic\ /\ Ptar}$) < Min (N_{low}) in category 1 or when Min ($N_{Pbic\ /\ Ptar}$) > Max (N_{high}) in category 2.

Non-parametric statistics (chi2-test) were then used to test whether frequencies of those categories differed (1) between genomic regions (supergene vs. rest of the genome) and (2) between transcripts where the level of expression was higher in P_{bic} / P_{bic} (category 1) *vs.* in P_{tar} / P_{tar} homozygotes (category 2).

Results

Patterns of expression between morphs differ within the supergene vs. the rest of the genome

Out of 53,224 genome-wide transcripts, we identified 5,855 transcripts with non-overlapping expression level between the two homozygous genotypes (*i.e.* 11% of all transcripts) (Table 1). Within the *P* inversion, we identified 141 transcripts with such non-overlapping expression between homozygotes, out of the 669 transcripts mapped to the supergene (*i.e.* 21% of the transcripts located within the supergene). Consistent with previous studies based on average expression (Saenko et al. 2019; Jay et al. 2021), genes with non-overlapping expression levels are enriched in the *P* inversion relatively to the rest of the genome (Chi^2 = 62.52, P < 0.001). At the genome-wide level, 2,798 and 3,057 transcripts are up-regulated in P_{bic} / P_{bic} and P_{tar} / P_{tar} homozygotes respectively, indicating a slight deviation toward up-regulation in P_{tar} / P_{tar} homozygotes (Chi^2 = 11.45, P < 0.001). However, within the *P* inversion, 56 and 39 transcripts are overexpressed in P_{bic} / P_{bic} and P_{tar} / P_{tar} homozygotes respectively. Interestingly, whereas differences in the *P* inversion does not deviate from parity (Chi^2 = 3.08, P = 0.079), it contrasts with genome-wide pattern (Chi^2 = 4.90, P = 0.027). A closer examination of the three subinversions P_1,

P_2 and P_3 revealed substantial differences. In the P_1 inversion, which is present in both homozygotes, overexpression of transcripts is more frequent in P_{bic} / P_{bic} than in P_{tar} / P_{tar} (30 vs. 7, respectively; Chi^2 = 14.30, P < 0.001)). An opposite pattern is found for P_2, where 4 and 13 transcripts are overexpressed in P_{bic} / P_{bic} and P_{tar} / P_{tar} homozygotes respectively (Chi^2 = 4.90, P = 0.029). For P_3 differentially expressed transcripts, no deviation from parity was observed with 22 and 19 up-expressed transcripts in P_{bic} / P_{bic} and P_{tar} / P_{tar} homozygotes respectively (Chi^2 = 0.22, P = 0.639). In fact, the difference in P_2 is even larger than the genome-wide pattern which also indicates an overexpression in P_{tar} / P_{tar} homozygotes (Chi^2 = 4.01, P = 0.045). In summary, the most important deviation from genome-wide pattern is biased towards P_{bic} / P_{bic} in P_1 and P_{tar} / P_{tar} in P_2.

A largely biased expression within the supergene toward P_{bic} / P_{bic} expression level in heterozygotes

When comparing genome-wide expression level in P_{bic} / P_{tar} heterozygotes to both homozygotes, we found that 997 and 739 transcripts showed expression level towards those of the P_{bic} / P_{bic} and P_{tar} / P_{tar}, respectively. This genome-wide pattern deviates from parity (Chi^2 = 38.34, P < 0.001) towards the expression pattern observed in the P_{bic} / P_{bic} homozygotes. Out of those transcripts, 25 and 5 in the P inversion showed expression level towards those of P_{bic} / P_{bic} and P_{tar} / P_{tar}, respectively (Figure 2). The pattern in the P inversion deviates from both parity (Chi^2 = 13.33, P < 0.001), as well as from the whole-genome pattern reflecting a 5-fold enrichment in the inversion (Chi^2 = 8.50, P = 3.55 x 10^{-3}). Interestingly and in contrast to comparisons between homozygotes, the three subinversions did not show any difference in their dominance pattern. Nevertheless, the most important departure from genome-wide homozygotes-based expectations being at P_2, with 6 and 1 heterozygous transcripts tending towards P_{bic} / P_{bic} and P_{tar} / P_{tar}, respectively (Chi^2 = 53.69, P < 0.001 despite low number of observations).

Further examination of dominance of gene expression in the P inversion revealed contrasting patterns between genes overexpressed in the two different homozygous genotypes

(Table 2). Whereas the 25 *bic*-dominant transcripts were almost equally distributed along the three subinversions P_1, P_2 and P_3, the 5 *tar*-dominant transcripts were all found at or near the inversion breakpoints. After rearranging the genomic regions according to the P_{tar} chromosome, all five transcripts located at the vicinity of the 200 kb long P_2 subinversion. Those five transcripts belonged to three genes and two intergenic regions, namely HMEL000021 and HMEL000024 (Sur-8) on P_1, an intergenic transcript close to HMEL032682 on P_2, and HMEL011885 (orthologous to *D. melanogaster* CG11414) and an intergenic transcript close to HMEL011882 on P_3. For the 25 *bic*-dominant transcripts, 11 belonged to intergenic regions whereas the remaining 14 transcripts belonged to 11 protein-coding genes. Two genes, namely HMEL000025 (*Cortex*) and HMEL000033 (Lmtk1, orthologous to *D. melanogaster Ddr*), had more than a single transcript. Both genes are on P_1 and are overexpressed in P_{bic} / P_{bic} homozygotes. Those multiple transcripts are most likely the result of alternative splicing. Another evidence for alternative splicing comes from a partial overlap (~10 bp) between an intergenic transcript (comp38651_c0_seq1) that is overexpressed in P_{bic} / P_{bic} and shows a *bic* dominance in the heterozygote and the HMEL000021 transcript which is overexpressed in P_{tar} / P_{tar} and shows a *tar* dominance in the heterozygote. When correcting for the P_1 inversion coordinates, these two overlapping transcripts with contrasting dominance patterns become adjacent to the P_1/P_2 breakpoint.

As indicated in the Methods above and Figure 2, we assigned signs to dominance estimates according to the overlap between the minimal counts of the heterozygotes relative to the intermediate expression between the two homozygous genotypes. For example, for a gene with a higher expression of the P_{bic} / P_{bic} homozygotes, dominance will be positive if the heterozygous minimal counts will be higher than the intermediate expression level and negative if it is below this threshold. The opposite trend follows for a gene with a higher expression in the P_{tar} / P_{tar} homozygotes. We therefore investigated whether the dominance observed on the transcripts of the heterozygotes was caused by an overexpression of these transcripts in one out of the two homozygote genotypes. We thus compared the number of dominant transcripts where an

overexpression was found in the P_{bic}/P_{bic} individuals (category 1) *vs.* the P_{tar}/P_{tar} homozygotes (category 2). At the genome-wide level, we indeed found an excess of transcripts for which expression levels in heterozygotes tend to follow the homozygous genotype with the highest expression level ($Chi^2 = 206.82$, $P < 0.001$). A similar trend was also found for genes in the ancestral P_1 inversion ($Chi^2 = 13.00$, $P < 0.001$). However, for both P_2 and P_3 inversions, there was no deviation from parity ($Chi^2 = 0.06$, $P = 0.806$) and the observed dominance patterns was thus not linked to an increased level of transcript expression in the P_{bic}/P_{bic} homozygous genotypes. This final observation indicates that nearly half of dominant transcripts in the two derived subinversions, P_2 and P_3, may be due to the downregulation of transcripts by the *bic* allele of genes that are overexpressed in the phenotypically recessive P_{tar} / P_{tar} homozygotes.

Discussion

Taken together our analyses of dominance of gene expression levels in *Heliconius* butterflies reveal that (1) expression levels of the transcripts in heterozygotes are more similar to the expression pattern observed in the dominant homozygous morph, (2) this dominance pattern is enriched but not restricted to the wing-pattern controlling *P* inversion, and (3) the most important deviation from homozygotes-based expectations is at the derived P_2 subinversion.

Genome wide pattern of expression confirms the switch role of the P *supergene.*

By comparing the genome-wide pattern of expression in pre-pupae with different genotypes at the supergene, we discovered important changes in transcript expressions. Genes in the supergene, such as the well-characterized gene *cortex* (Nadeau et al. 2016) located in the P_1 subinversion, may regulate cascades of wing patterning and melanin synthesis genes found outside the *P* region, changing gene expression in multiple loci throughout the genome. Our study focused on the prepupal stage, where the pre-patterning of the wing starts to be expressed, and the *P* supergene probably behaves as a switch locus, acting upstream of the genetic pathways inducing

variation in wing colour pattern development. Consistent with this hypothesis, at the genome scale, the transcript expression patterns in the heterozygotes at the supergene is biased towards the expression observed in the dominant P_{bic}/P_{bic} rather than in the P_{tar}/P_{tar}. This biased expression pattern at the pre-pupal stage may indeed contributes to the development of the *bicoloratus* wing colour pattern in P_{tar}/P_{bic} heterozygous imago. Many genes identified as causing colour pattern variations are indeed transcriptional factors that may have a pleiotropic, upstream effect in the colour pattern development pathway, rather than a downstream effect. For instance, the signaling gene *WntA*, that plays a major role in colour pattern variation in butterflies, is thought to act as a major pre-patterning element, rather than a downstream gene determining the final identity of wing scales (Martin and Reed 2014).

Heterozygous patterns of expression in the P *region suggests a combination of molecular mechanisms involved in coordinated phenotypic dominance.*

Our approach focused on the detection of non-additive patterns of transcript expression. Nevertheless, assuming a threshold above which a certain developmental pathway is triggered, intermediate expression of a transcript in heterozygotes might be sufficient to generate dominance (Gilchrist and Nijhout 2001). Here, we focused on the deviation from additivity, therefore identifying biased patterns of expression of transcript in the heterozygotes, which might represent only a fraction of the molecular mechanisms involved in phenotypic dominance. In the P_1 subinversion, there is a strong overexpression of transcripts in the P_{bic}/P_{bic} homozygotes as compared to P_{tar}/P_{tar} homozygotes. This high expression level in the P_1 region is also found in the P_{bic}/P_{tar} heterozygotes, suggesting that high level of P_1 transcripts might trigger the development of the *bicoloratus* phenotype. The identification of upregulated transcripts in the *cortex* gene might play a major role in the developmental switch between *tarapotensis* and *bicoloratus*. Interestingly, the downregulation in heterozygotes of transcripts belonging to the P_2 subinversion, that are otherwise overexpressed in the recessive *tarapotensis* morph might also contribute to the

development of the *bicoloratus* phenotypes. Such downregulation might be promoted by selection acting on the dominance at the *P* supergene, contributing to the coordinated pattern of dominance observed in sympatric homozygotes (Le Poul et al. 2014). If such a hypothesis turns out to be correct, this would indicate that the evolution of complex dominance patterns in *Heliconius* may have involved a step-wise process, with (1) a Haldane's sieve-like evolution of a dominant derived allele at $P_{1,}$ where the over-expression of the dominant transcripts drive phenotypic development towards the *bicoloratus* phenotype and (2) the evolution of repression in the genes located in the younger sub-inversions P_2 and P_3, preventing the expression of the transcripts triggering the development of the recessive *tarapotensis* phenotypes. This study thus represents a promising step towards the understanding of the evolution of dominance relationships in complex phenotypic traits. Investigating the pattern of different heterozygous combinations at the *P* supergene would certainly shed light on the different molecular mechanisms causing the coordinated dominance observed at the phenotypic scale, allowing to reconstruct the evolutionary history of dominance relationships.

Candidate genes for the development of colour pattern with multiple elements

The *bicoloratus* and *tarapotensis* colour pattern phenotypes differ in a number of melanic and yellow elements, that might be controlled by different genetic bases. The identification of contrasted patterns of expression in the different transcripts within the supergenes in heterozygotes may shed light on the genetic architecture controlling variations of such a complex colour pattern. Out of the 669 transcripts of the 2 Mb-long *P* inversion, our analysis identified only 30 candidate transcripts, and therefore represents a significant step towards the identification of the molecular basis of dominance evolution in this important model of adaptive polymorphism. Although the functional role of these different genes on wing pattern development is not obvious, the genes for which heterozygotes have a biased expression toward the P_{bic} / P_{bic} expression level can be putative candidates for the developmental switch between *tarapotensis* and *bicoloratus* colour patterns. Note that these genes did not display any signal of differential expression when we compared expression

levels across homozygotes (Saenko et al. 2019). Nevertheless, a switch in developmental pathway can be triggered by variations in the levels of certain signaling proteins but can also be triggered by variations in the protein sequence. We thus hope our study will stimulate larger-scale investigation of expression patterns, allowing to refine our knowledge on the combinations of genetic elements involved in such major developmental switch.

Acknowledgments

This study was funded by ANR JCJC *DOMEVOL* and the Emergence program of Paris City council to VL and by ANR *SUPERGENE* to MJ.

Conflict of Interest

The authors declare that they have no conflict of interest.

Data Archiving

The data can be found in the NCBI SRA and TSA repositories under the number PRJNA555830.

References

Arias M, le Poul Y, Chouteau M, Boisseau R, Rosser N, Théry M et al. (2016) Crossing fitness valleys: empirical estimation of a fitness landscape associated with polymorphic mimicry. Proc R Soc B 283:20160391.

Billiard S, Castric V, Llaurens V (2021) The integrative biology of genetic dominance. Biol Rev 96:2925–2942.

Challi RJ, Kumar S, Dasmahapatra KK, Jiggins CD, Blaxter M (2016) Lepbase: the Lepidopteran genome database. bioRxiv:056994.

Charlesworth B, Charlesworth D (1999) The genetic basis of inbreeding depression. Genet Res 74:329–340.

Charlesworth D, Willis JH (2009) The genetics of inbreeding depression. Nat Rev Genet 10:783–796.

Chouteau M, Arias M, Joron M (2016) Warning signals are under positive frequency-dependent selection in nature. PNAS 113:2164–2169.

Connallon T, Hall MD (2018) Genetic constraints on adaptation: a theoretical primer for the genomics era. Ann NY Acad Sci 1422:65–87.

Durand E, Méheust R, Soucaze M, Goubet PM, Gallina S, Poux C et al. (2014) Dominance hierarchy arising from the evolution of a complex small RNA regulatory network. Science 346:1200–1205.

Gilchrist MA, Nijhout HF (2001) Nonlinear developmental processes as sources of dominance. Genetics 159:423-432.

Haas BJ, Papanicolaou A, Yassour M, Grabherr M, Blood PD, Bowden J et al. (2013) *De novo* transcript sequence reconstruction from RNA-seq using the Trinity platform for reference generation and analysis. Nat Protoc 8:1494–1512.

Haldane JBS (1956) The theory of selection for melanism in Lepidoptera. Proc R Soc Lond B 145:303–306.

Jay P, Whibley A, Frézal L, Rodríguez de Cara MÁ, Nowell RW, Mallet J et al. (2018) Supergene evolution triggered by the introgression of a chromosomal inversion. Curr Biol 28:1839-1845.

Jay P, Chouteau M, Whibley A, Bastide H, Parrinello H, Llaurens V et al. (2021) Mutation load at a mimicry supergene sheds new light on the evolution of inversion polymorphisms. Nat Genet 53:288–293.

Jay P, Leroy M, Le Poul Y, Whibley A, Arias M, Chouteau M et al (2022) Association mapping of colour variation in a butterfly provides evidence that a supergene locks together a cluster of adaptive loci. Philos Trans R Soc B 377:20210193.

Joron M, Frezal L, Jones RT, Chamberlain NL, Lee SF, Haag CR et al. (2011) Chromosomal rearrangements maintain a polymorphic supergene controlling butterfly mimicry. Nature 477:203–206.

Joron M, Papa R, Beltrán M, Chamberlain N, Mavárez J, Baxter S et al. (2006) A conserved supergene locus controls colour pattern diversity in Heliconius butterflies. PLOS Biol 4:e303.

Joron M, Wynne IR, Lamas G, Mallet J (1999) Variable selection and the coexistence of multiple mimetic forms of the butterfly Heliconius numata. Evol Ecol 13:721–754.

452 Langmead B, Salzberg SL (2012) Fast gapped-read alignment with Bowtie 2. Nat Method 9:357–
453 359.

454 Le Poul Y, Whibley A, Chouteau M, Prunier F, Llaurens V, Joron M (2014) Evolution of
455 dominance mechanisms at a butterfly mimicry supergene. Nat Commun 5:1–8.

456 Li H, Handsaker B, Wysoker A, Fennell T, Ruan J, Homer N et al. (2009) The Sequence
457 Alignment/Map format and SAMtools. Bioinformatics 25:2078–2079.

458 Livraghi L, Hanly JJ, Loh LS, Ren A, Warren IA, Concha C et al. (2020) The gene *cortex* controls
459 scale colour identity in Heliconius. bioRxiv:2020.05.26.116533.

460 Llaurens V, Billiard S, Castric V, Vekemans X (2009) Evolution of dominance in sporophytic self-
461 incompatibility systems: I. Genetic load and coevolution of levels of dominance in pollen
462 and pistil. Evolution 63:2427–2437.

463 Llaurens V, Joron M, Billiard S (2015) Molecular mechanisms of dominance evolution in Müllerian
464 mimicry. Evolution 69:3097–3108.

465 Martin M (2011) Cutadapt removes adapter sequences from high-throughput sequencing reads.
466 EMBnet.journal 17:10–12.

467 Martin A, Reed RD (2014) *Wnt* signaling underlies evolution and development of the butterfly wing
468 pattern symmetry systems. Dev Biol 395:367-378.

469 Martin A, Papa R, Nadeau NJ, Hill RI, Counterman BA, Halder G et al. (2012) Diversification of
470 complex butterfly wing patterns by repeated regulatory evolution of a *Wnt* ligand. PNAS
471 109:12632–12637.

472 Nadeau NJ, Pardo-Diaz C, Whibley A, Supple MA, Saenko SV, Wallbank RWR et al. (2016) The
473 gene *cortex* controls mimicry and crypsis in butterflies and moths. Nature 534:106–110.

Otto SP, Bourguet D (1999) Balanced polymorphisms and the evolution of dominance. Am Nat 153:561-574.

Saenko SV, Chouteau M, Piron-Prunier F, Blugeon C, Joron M, Llaurens V (2019) Unravelling the genes forming the wing pattern supergene in the polymorphic butterfly *Heliconius numata*. EvoDevo 10:16.

Schmieder R, Edwards R (2011) Quality control and preprocessing of metagenomic datasets. Bioinformatics 27:863–864.

Schmieder R, Lim YW, Edwards R (2012) Identification and removal of ribosomal RNA sequences from metatranscriptomes. Bioinformatics 28:433–435.

Wilkie AO (1994) The molecular basis of genetic dominance. J Med Genet 31:89–98.

Yamamoto F, Clausen H, White T, Marken J, Hakomori S (1990) Molecular genetic basis of the histo-blood group ABO system. Nature 345:229–233.

Yassin A, Bastide H, Chung H, Veuille M, David JR, Pool JE (2016) Ancient balancing selection at tan underlies female colour dimorphism in *Drosophila erecta*. Nat Commun 7:10400.

Tables

Table 1: Classification of transcripts with non-overlapping expression difference between homozygous genotypes. The categories are based on the sign of the dominance value, with $D > 0$ indicating expression level in the heterozygote approaching that of the P_{bic} / P_{bic} homozygous genotype. Whole-genome refers to all RNA-Seq transcripts that do not map to the *P* inversion. *P1*, *P2* and *P3* refer to the three subinversions after Jay et al. (2021).

Category	Whole-genome	*P*	P_1	P_2	P_3
C1: Min($N_{Pbic\ /\ Pbic}$) > Max($N_{Ptar\ /\ Ptar}$)	2742	56	30	4	22
$D > 0$ (*bic*-dominant)	619	17	11	1	5
$D < 0$ (*tar*-dominant)	203	1	0	0	1
C2: Min($N_{Ptar\ /\ Ptar}$) > Max($N_{Pbic\ /\ Pbic}$)	3018	39	7	13	19
$D > 0$ (*bic*-dominant)	353	8	0	5	3
$D < 0$ (*tar*-dominant)	531	4	2	1	1

Table 2: Overview of the 25 *bic*-dominant ($D>0$) and 5 *tar*-dominant transcripts ($D<0$) along the P_1, P_2 and P_3 subinversions. AS indicates the potential presence (+) or absence (-) of alternative splicing. Categories refer to whether the transcript was over-expressed in the P_{bic} / P_{bic} (B) or the P_{tar} / P_{tar} (T) genotypes (see Materials and Methods).

subinversion	Transcript ID	Hmel gene	scaffold	Start	end	category	*D*	AS
P_1	comp38651_c0_seq1	Intergenic	215006	1137280	1137877	B	2	+
	comp46151_c0_seq2	HMEL000021	215006	1137867	1138685	T	-2	+
	comp371181_c0_seq1	HMEL000024	215006	1149611	1149345	T	-2	-
	comp45148_c0_seq1	HMEL000025	215006	1205192	1205467	B	2	+
	comp45148_c0_seq2	HMEL000025	215006	1205192	1205467	B	2	+
	comp47446_c0_seq1	HMEL000026	215006	1386784	1387136	B	2	-
	comp48116_c0_seq1	HMEL000033	215006	1448480	1444964	B	2	-
	comp46606_c0_seq2	HMEL000033	215006	1452848	1451680	B	2	-
	comp44351_c0_seq1	HMEL000033	215006	1464644	1463551	B	2	-
	comp42021_c0_seq1	Intergenic	215006	1465392	1465112	B	2	-
	comp37963_c0_seq1	Intergenic	215006	1467433	1466204	B	2	-
	comp39322_c0_seq1	HMEL032680	215006	1470290	1470648	B	2	+
	comp39322_c0_seq2	HMEL032680	215006	1470468	1470648	B	2	+
P_2	comp77610_c0_seq1	Intergenic	215006	1524826	1524452	T	-2	-
	comp29763_c0_seq1	HMEL000040	215006	1546728	1547707	B	3	-
	comp18312_c0_seq1	HMEL000043	215006	1559504	1558901	T	2	-
	comp57308_c0_seq1	Intergenic	215006	1559809	1559596	T	2	-
	comp16331_c0_seq1	Intergenic	215006	1560330	1560025	T	2	-
	comp65172_c0_seq1	Intergenic	215006	1562334	1562034	T	2	-
	comp51564_c0_seq1	Intergenic	215006	1562989	1562450	T	2	-
P_3	comp34931_c0_seq1	Intergenic	215006	1732081	1731708	B	2	-
	comp16734_c0_seq1	Intergenic	215006	1733144	1732720	B	2	-
	comp45413_c0_seq1	HMEL015101	215008	72354	70218	B	2	-
	comp45063_c0_seq1	HMEL013484	215008	205484	205150	T	2	-
	comp18410_c0_seq1	Intergenic	215009	11292	10610	T	2	-
	comp35260_c0_seq1	HMEL021462	215012	9348	9091	B	2	-
	comp11639_c0_seq1	HMEL022056	215024	1147	1355	T	2	-
	comp49598_c0_seq1	Intergenic	215025	59298	59741	B	-2	-
	comp40013_c0_seq1	HMEL011884	215025	68170	67093	B	2	-
	comp39620_c0_seq1	HMEL011885	215025	70515	70880	T	-2	-

519 **Figure legends**

520

521 Figure 1: A. Patterns of wing coloration in the *bicoloratus* (*bic*) and *tarapotensis* (*tar*) morphs of
522 the species *Heliconius numata* and their co-mimics from the genus *Melinaea*. The diversity in wing
523 pigmentation is associated with a dominance relationship between the two morphs: wing colour
524 pattern of the P_{bic} / P_{tar} heterozygotes show a striking similarity with the colour pattern of P_{bic} / P_{bic}
525 homozygotes except at two spots (blue arrows). B. Three series of inversion at the supergene are
526 associated with the two morphs *bic* and *tar* (Jay et al. 2021). The rearrangement P_1 involves an
527 event of inversion that spans over 400 kb and is associated with the phenotype *bicoloratus*. P_2 and
528 P_3 involve two supplementary inversions of roughly 0.2 and 1.2 Mb respectively and are associated
529 here with the phenotype *tarapotensis*.

530

531 Figure 2: Quantification scheme of the degree of dominance (*D*) in the expression level of
532 transcripts. Two categories of transcripts were considered, depending on the levels of expression in
533 the P_{bic}/P_{bic} and P_{tar} / P_{tar} homozygotes (category 1: when $Min(N_{Pbic\,/\,Pbic}) > Max(N_{Ptar\,/\,Ptar})$ and
534 category 2 when $Min(N_{Ptar\,/\,Ptar}) > Max(N_{Ptbic/\,Pbic})$. The dominance score was assessed depending on
535 the minimum and maximum number of transcripts observed in the different replicates (represented
536 by the transparent boxes) of the same homozygous (in red and blue) and heterozygous (in purple)
537 genotypes (see Methods). A score ranging from -3 to 3 was then given to each transcript following
538 its class in respect to the phenotypically-dominant P_{bic} / P_{bic} homozygous genotype.

539

540 Figure 3: Distribution of *D* values based on level of gene expression along the supergene (see text
541 and Fig. 2 for quantification scheme). Gray dots refer to transcripts with overlapping expression
542 between the homozygous genotypes or between the homozygotes and the heterozygote. Transcripts
543 with non-overlapping expression levels between the homozygous genotypes are indicated in violet
544 and turquoise colors according to whether the expression was higher in the P_{bic} / P_{bic} (category 1) or

545 P_{tar} / P_{tar} homozygous genotype (category 2), respectively. Vertical lines indicate borders of the
546 three subinversions according the Hmel2 reference genome coordinates of chromosome 15.
547

A

Melinaea
Model species

Heliconius numata
Mimetic species

Melinaea marsaeus mothone

Heliconius numata bicoloratus

bic/bic

bic/tar

tar/tar

Melinaea menophilus ssp. nov.

Heliconius numata tarapotensis

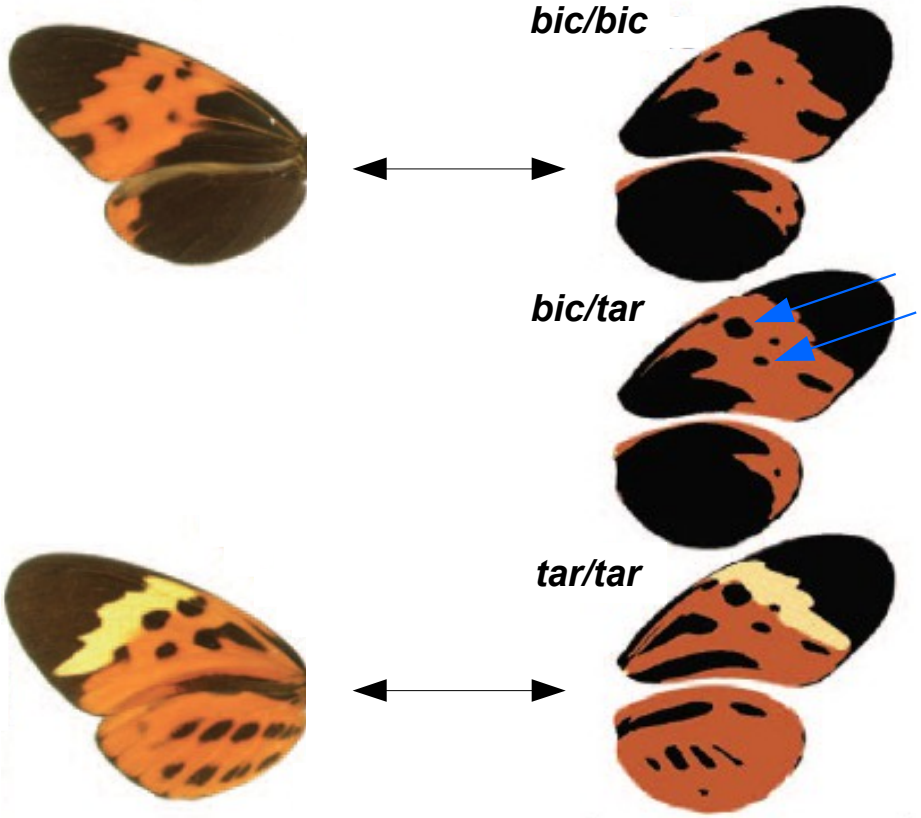

B

Chromosomal rearrangements at the supergene

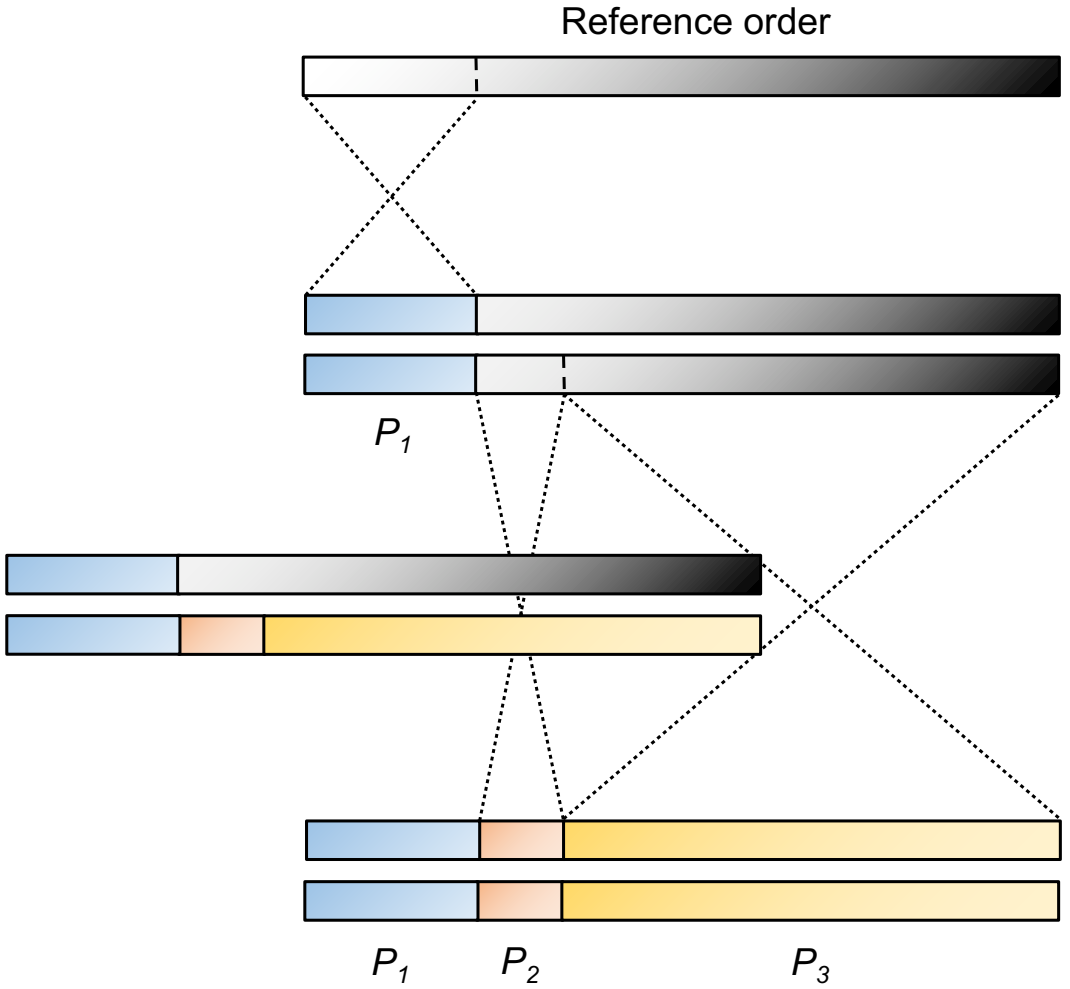


Category 1
bic/bic > tar/tar
tar/tar
bic/bic
bic/tar
D
-3
-2
-1
0
1
2
3
Number of transcripts
max (N_high)
min (N_high)
additivity
max (N_low)
min (N_low)
Category 2
tar/tar > bic/bic
Number of transcripts
max (N_high)
min (N_high)
additivity
max (N_low)
min (N_low)
Increasing level of dominance of the bic allele

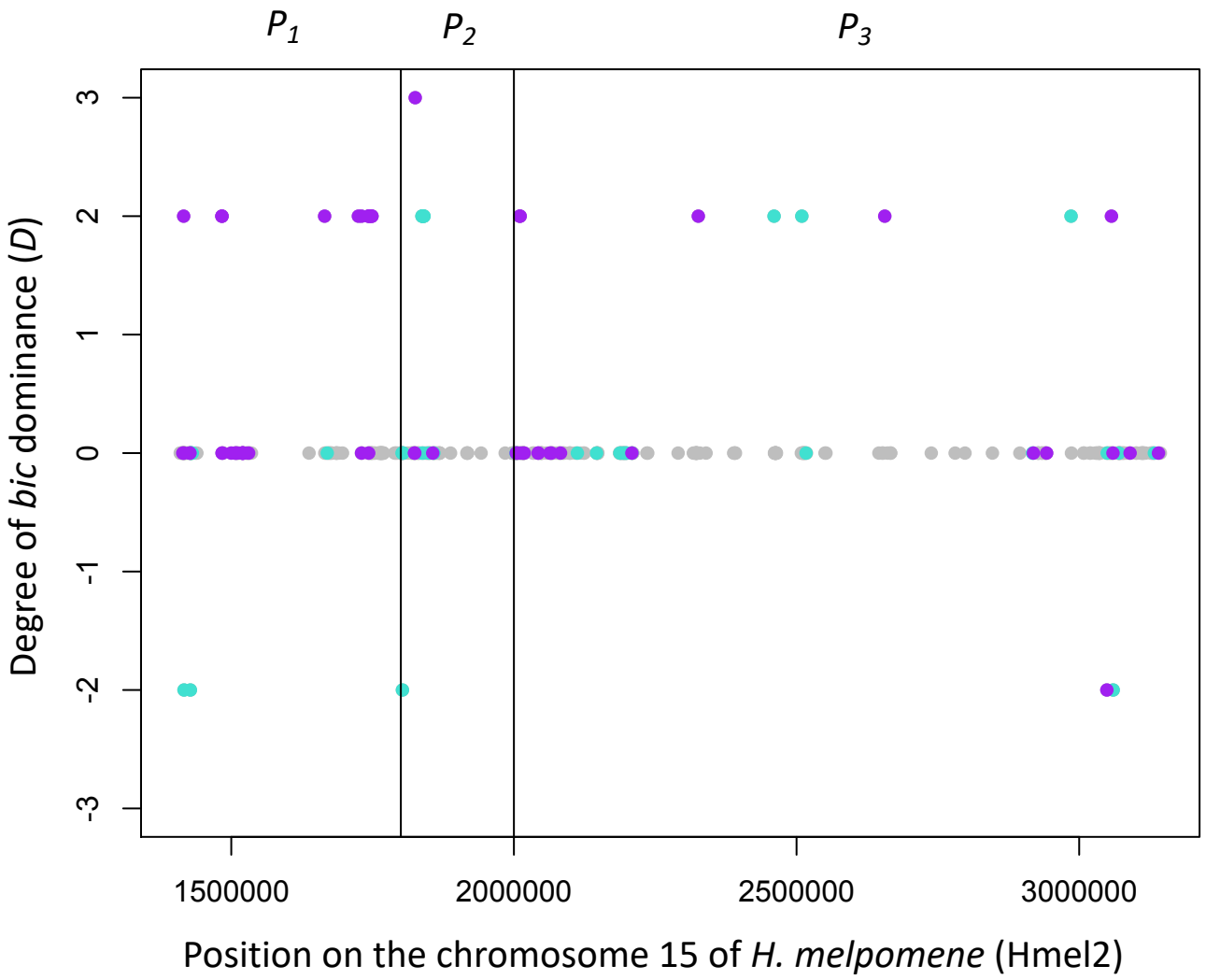
P_1
P_2
P_3
Degree of *bic* dominance (*D*)
3
2
1
0
-1
-2
-3
1500000
2000000
2500000
3000000
Position on the chromosome 15 of *H. melpomene* (Hmel2)